RESEARCH ARTICLE

VOL. 43 | NO. 3 | **SEPTEMBER - DECEMBER 2022** | PP 25-35

Revista Mexicana de Ingeniería Biomédica

dx.doi.org/10.17488/RMIB.43.3.3

E-LOCATION ID: 1298

Electrical Impedance Tomography to Measure Spirometry Parameters in Chronic Obstructive Pulmonary Disease Patients

Tomografía por Impedancia Eléctrica para Medir Parámetros de Espirometría en Pacientes con Enfermedad Pulmonar Obstructiva Crónica

Francisco Miguel Vargas Luna[1], *Svetlana Kashina*[1], *Pere Joan Riu Costa*[2], *Pere Casan Clarà*[3], *José Marco Balleza Ordaz*[1]

[1]División de Ciencias e Ingenierías, Universidad de Guanajuato, Campus León - Guanajuato, Mexico

[2]Universidad Politécnica de Cataluña - Barcelona, Spain

[3]Research Institute of the Principality of Asturias, ISPA, University of Oviedo - Oviedo, Spain

ABSTRACT

Spirometry is a test for the diagnosis of chronic obstructive pulmonary disease. It is a technique that can be intolerant due to the essential use of a mouthpiece and a clamp. This study proposes the use of electrical impedance tomography to measure respiratory parameters. Patients underwent spirometry and three respiratory exercises. The impedance signals were convolved, and the resultant was analyzed by fast Fourier transform. The frequency spectrum was divided into seven segments (R1 to R7). Each segment was represented in terms of quartiles (Q25%, Q50%, Q75%). Each quartile of each segment was correlated with the spirometric parameters to obtain a fitting equation. FVC was correlated 70% with the 3 quartiles of R7, 3 equations were obtained with a fit of 60%. FEV1 correlated 70% with the Q50% of R7, obtaining an equation with a fit of 40%. FEV1/FVC correlated 69% with Q75% of R2, obtaining an equation with a fit of 60%. Spirometric parameters can be estimated from the implied carrier frequency components of the ventilatory impedance signal.

KEYWORDS: Electrical impedance tomography, respiration, spirometry, calibration, monitoring

RESUMEN

La espirometría es una prueba para el diagnóstico de enfermedad pulmonar obstructiva crónica. Es una técnica que puede resultar intolerante debido al uso imprescindible de una boquilla y una de pinza. Este estudio propone el uso de la tomografía de impedancia eléctrica para medir los parámetros respiratorios. Los pacientes realizaron una espirometría y tres ejercicios respiratorios. Las señales de impedancia fueron convolucionadas, y la resultante se analizó mediante una transformada rápida de Fourier. El espectro en frecuencias se dividió en siete segmentos (R1 a R7). Cada segmento se representó en términos de cuartiles (Q25%, Q50%, Q75%). Cada cuartil de cada segmento se correlacionó con los parámetros espirométricos para obtener una ecuación de ajuste. La FVC se correlacionó en un 70% con los 3 cuartiles de R7, se obtuvieron 3 ecuaciones con un ajuste del 60%. El FEV1 se correlacionó en un 70% con el Q50% de R7, obteniéndose una ecuación con un ajuste del 40%. El FEV1/FVC se correlacionó en un 69% con el Q75% de R2, obteniéndose una ecuación con un ajuste del 60%. Los parámetros espirométricos pueden ser estimados a partir de los componentes de frecuencia portadora implícitos de la señal de impedancia ventilatoria.

PALABRAS CLAVE: Tomografía por la impedancia eléctrica, respiración, espirometría, calibración, monitorización

Corresponding author

TO: José Marco Balleza Ordaz

INSTITUTION: División de Ciencias e Ingenierías, Universidad de Guanajuato - Campus León

ADDRESS: Lomas del Bosque #103, Col. Lomas del Campestre, C. P. 37150, León, Guanajuato, México

CORREO ELECTRÓNICO: jm.balleza@ugto.mx

Received:

10 August 2022

Accepted:

20 October 2022

INTRODUCTION

Currently, mortality caused by chronic respiratory tract diseases is increasing in Mexico and occupied the fourth position in 2020. Chronic obstructive pulmonary disease (COPD) deaths are 2.49% of total mortality nationwide [1]. According to the Global Initiative for Chronic Obstructive Lung Disease, COPD showed a worldwide prevalence of 3.92% in 2017 (95% CI 3.52% - 4.32%). In 2021, the estimated global mortality rate was 42/100,000 (4.72%) and the DALY (Disability Adjusted Life Years) rate was 1068.02/100,000 inhabitants [2]. COPD is a common, preventable, and treatable disease characterized by persistent respiratory symptoms and airflow limitation due to airway and/or alveolar abnormalities, usually caused by significant exposure to noxious agents [2] [3]. The initial procedure for diagnosing COPD is spirometry, which is a non-invasive technique that measures the volume of air that the lungs can mobilize as a function of time [2] [3] [4]. However, the technique may be intolerant to the patient because of the use of a mouthpiece and nose clip, and the specific respiratory maneuver to be performed [5] [6] [7].

Vogt *et a*l [8] proposed the use of EIT to visualize the pulmonary ventilatory distribution (PVD) in a group of 35 COPD patients under the influence of an inhaled bronchodilator. Monitoring was performed immediately after inhalation and at 5, 10, and 20 minutes.

Signals from the EIT system and an electronic spirometer were recorded simultaneously. PVD was assessed by estimating the changes in impedance corresponding to the parameters: forced expiratory volume in 1 second (FEV1), forced vital capacity (FVC), pulmonary circulating volume (VC), peak flow (PF), and forced expiratory flow between 25 % and 75% of the FVC (FEF25-75%). The FEV1/FVC parameter was estimated from the elements of the EIT image to assess the post-bronchodilator effect in a regional manner. Only 17 showed a significant bronchodilator response. The FEV1 parameter and CV changes showed significant correlations with the impedance changes of the regions of interest of the EIT images in patients with bronchodilator response [8].

Due to the above, this work proposes the use of the electrical impedance tomography (EIT) technique to measure the FVC, FEV1, and FEV1/FVC parameters from the respiratory recording obtained by EIT, analyzing the frequency components implicit in the changes in lung tidal volume. The objective of this study is to obtain a set of mathematical calibration models that adjust the module's frequency components powers (dB) and the phase of the impedance signal due to lung tidal volume obtained by EIT, to estimate the FVC, FEV1, and FEV1/FVC parameters.

MATERIALS AND METHODS

Pneumotachograph

Circulating volume measurements were obtained by a MedGraphics prevent TM Pneumotach kit (St. Paul, MN, USA). This system allows continuous recording of flow and time signals, both graphically and numerically. According to the standardized protocol, calibration was performed using a 3L syringe [9].

Electrical Impedance Tomography (EIT)

EIT was carried out with the TIE4sys system, experimental equipment designed by the Electronic Engineering Department of the Universitat Politècnica de Catalunya, Barcelona, Spain. The equipment uses 16 electrodes (Red Dot 2560 - 3 M, London, Ontario, Canada) placed around the chest, following the standardized protocol [10]. The calibration of the EIT system was performed on an arrangement of electrical resistance of 330 ohms as described in [11]. TIE4sys acquires 17 images/s and applies an alternating electrical current of 1 mA at 48 kHz through two adjacent electrodes. A differential voltage is detected across a pair of electrodes whose position is moved adjacently across the main 16-electrode array. Once the voltage measurement cycle is finished, the injector pair moves to its adjacent position, starting a new measurement cycle. The measurement cycle ends when all electrodes have been used as current injectors and voltage detectors [11] [12]. EIT images are obtained using a weighted back-projection reconstruction algorithm. The EIT images are referential, a reference image is used to obtain subsequent images. This is reconstructed by obtaining and averaging 200 images corresponding to a lapse of 12 seconds of breathing [13].

Participants

A group of 15 patients diagnosed with COPD was analyzed. A spirometry test was performed and forced vital capacity (FVC), forced expiratory volume in 1 second (FEV1), and the ratio of the above parameters (FEV1/FVC) was also recorded. The examinations were carried out between 9:00 a.m. and 12:00 p.m. in a room with an ambient temperature of 25°C, 60% humidity, and at sea level. All of them voluntarily agreed to participate in the study, which had been previously approved by the center's Ethics Committee (Comité de Ética de la Secretaría de Salud del Estado de Guanajuato, México, del Hospital General de León, Approval Folio Number: GTSSA002101-364).

Procedure

The pneumotachometer and the TIE4sys were simultaneously connected to each participant. Changes in the participants' circulating volume were recorded over 30 s, with a 3-min break between measurements. The number of cycles recorded for each individual varied between 20 and 25. For each respiratory exercise, 510 impedance measurements were recorded. In this study, three respiratory maneuvers per patient were acquired.

The data were analyzed and processed using the Python computer program [14]. A convolution of the three respiratory signals was performed [15]. In this case, the product of the first two signals was obtained and the resulting signal was convolved with the third, obtaining the analysis signal. Subsequently, the resulting signal was analyzed by applying the Fast Fourier Transform (FFT). FFT is a mathematical process that transforms any time-varying signal into a frequency spectrum (FS) [16]. The FS was reconstructed with 182 data, dividing it into seven segments (from R1 to R7), each with 26 data, the minimum statistically significant amount to be analyzed independently. Segment R1 was defined between 0-117.49mHz, R2 between 156.66mHz-274.15mHz, R3 between 313.32mHz-430.18mHz, R4 between 469.98mHz-587.47mHz, R5 between 626.64mHz-744.13mHz, R6 between 783.30mHz-900. mHz and R7 between 939.95mHz-1.06Hz. The area under the curve (AuC) was estimated for each segment. The AuC is used to normalize the estimates of means or quartiles of each segment.

Statistical analysis

The normal distribution of the data of each frequency segment was analyzed using the Shapiro-Wilk statistical test (S-W, significance value $p<0.05$). The correlation between the means and the FVC, FEV1, and FVC/FEV1 parameters was performed using the Pearson statistical test, establishing a significance of $p<0.05$. The correlation between the quartiles and the FVC, FEV1, and FVC/FEV1 parameters was performed through the Spearman statistical test, establishing a significance of $p<0.05$. The mathematical models to determine the spirometry parameters either in terms of means (S-W with $p>0.05$) or quartiles (S-W with $p<0.05$) were obtained from linear regression, establishing a coefficient of determination R2>0.5. The validation of the obtained data is carried out in case the S-W is greater than 0.05, by means of the T-test for paired data. Otherwise, it is done using the Wilcoxon test. In these tests, a level of significance $p>0.05$ was established.

Differences in results were analyzed using a Bland and Altman plot [17].

RESULTS AND DISCUSSION

Normality analysis and data representation

The data of the FVC, FEV1 and FEV1/FVC parameters evidenced a normal distribution (S-W $p>0.05$), therefore, they are represented in terms of means (±SD). The power determinations of the seven frequency segments did not show a normal distribution (S-W $p<0.05$), so, they are represented in terms of 25%, 50%, and 75% quartiles. Statistical analysis of these data was performed with Spearman's correlation coefficient and Wilcoxon's test.

The mean values of FVC, FEV1 and FEV1/FVC were 70%±14%, 46%±12%, and 46%±7%, respectively. The distribution of the powers corresponding to the seven frequency segments obtained from the module and phase are shown in Table 1.

TABLE 1. Distribution of the powers (in decibels, dB) of the seven frequency segments that make up the changes in pulmonary ventilation obtained by EIT corresponding to the 15 patients with COPD.

FOI[1] (mHz)	Impedance Module Powers (dB)				Phase Module Powers (dB)			
	Quartile at	Q25%[2]	Q50%[3]	Q75%[4]	Quartile at	Q25%[2]	Q50%[3]	Q75%[4]
0* – 117.49	25%	0.107	0.201	0.279	25%	0.070	0.125	0.306
	50%	0.282	0.309	0.332	50%	0.297	0.333	0.339
	75%	0.373	0.506	0.675	75%	0.388	0.530	0.635
156.66 – 274.15	25%	0.041	0.100	0.135	25%	0.114	0.210	0.248
	50%	0.214	0.292	0.317	50%	0.310	0.330	0.337
	75%	0.479	0.567	0.697	75%	0.433	0.468	0.505
313.32 – 430.18	25%	0.048	0.088	0.164	25%	0.151	0.212	0.290
	50%	0.152	0.211	0.279	50%	0.312	0.330	0.335
	75%	0.523	0.609	0.731	75%	0.376	0.428	0.567
469.98 – 587.47	25%	0.067	0.116	0.207	25%	0.249	0.293	0.314
	50%	0.189	0.271	0.337	50%	0.326	0.333	0.357
	75%	0.509	0.649	0.736	75%	0.350	0.372	0.466
626.64 – 744.13	25%	0.114	0.212	0.258	25%	0.147	0.267	0.314
	50%	0.279	0.312	0.346	50%	0.304	0.333	0.339
	75%	0.396	0.477	0.604	75%	0.359	0.441	0.579
783.30 – 900.79	25%	0.208	0.254	0.289	25%	0.231	0.287	0.306
	50%	0.294	0.331	0.342	50%	0.324	0.333	0.335
	75%	0.371	0.411	0.451	75%	0.352	0.381	0.425
939.95 – 1060	25%	0.239	0.261	0.307	25%	0.220	0.254	0.315
	50%	0.301	0.332	0.340	50%	0.331	0.333	0.343
	75%	0.354	0.391	0.462	75%	0.363	0.414	0.487

[1]FOI: Frequencies of Interest, seven frequency segments in mHz expressed in terms of powers (decibels, dB). The dispersion of these powers is expressed in terms of quartiles (25%, 50%, and 75%) because these data do not show a normal distribution.
[2]Q25%, 25% quartile of power data.
[3]Q50%, 50% quartile of power data.
[4]Q75%, 75% quartile of power data.
*- zero indicates theoretical value.

Correlations between spirometry parameters and powers of frequency segments

In the case of the frequency components of the impedance module, significant correlations of approximately 70% were found between: 1) the three quartiles of frequency segment 7 and the FVC; 2) between the 50% quartile of segment 7 and FEV1; and 3) the 75% quartile of frequency segment 2 and the FEV1/FVC. In the case of the frequency components of the impedance phase, significant correlations of approximately 60% were found between the 25% and 75% quartiles of segments 4 and 7 and the FVC, respectively; and a correlation greater than 70% between the 25% and 75% quartiles of segment 4 and FEV1 (Table 2).

TABLE 2. Correlations between the powers of the frequency components of the impedance module and phase signals and the spirometric parameters.

Powers of the frequency components of the module signal and spirometric parameters					Powers of the frequency components of the phase signal and spirometric parameters			
FOI[1]	Quartile at	FVC[2]	FEV1[3]	FEV1/FVC[4]	FOI[1]	Quartile at	FVC[2]	FEV1[3]
S7	25%	-0.682	-	-	S4	25%	-0.632	-0.737
	50%	-0.731	-0.732	-		75%	0.646	0.789
S2	75%	0.693	-	-	S7	25%	-0.600	-
	75%	-	-	-0.698		75%	0.661	-

[1]FOI: frequencies of interest: S2 – Segment 2 (156.66 – 274.15 mHz), S4 – Segment 4 (469.98 – 587.47 mHz), S7 – Segment 7 (939.95 mHz – 1.06 Hz).
[2]FVC: forced vital capacity.
[3]FEV1: forced expiratory volume in the first second.
[4]FEV1/FVC: quotient between the parameters FEV1 and FVC.

Mathematical fit models

Five equations were obtained that adjust the powers of the impedance signal module to estimate the 3 spirometry parameters. Three determine the estimation of the FVC, one - the FEV1 and the rest - the FEV1/FVC. The mean value of the coefficient of determination (R2) of the 5 equations was approximately 54%±11% (Table 3).

Six equations were obtained that adjust the phase powers to estimate two spirometry parameters. Four of these determine the estimation of the FVC and two of the FEV1. The mean value of the R2 of the 5 equations was approximately 33%±16% (Table 3).

Evaluation of mathematical fit models

The correlation between measured and estimated determinations for FVC, FEV1, and FEV1/FVC was approximately 76% (p<0.001), 65% (p<0.001), and 69% (p<0.001), respectively (Table 4).

The average value of the dispersion of the measured FVC, FEV1 and FEV1/FVC determinations and those estimated with the impedance modulus equations (Table 3) were 11% (T-Student p=0.903, acceptability at 95%: ±18 %), 19% (T-Student p=0.957, acceptability at 95%: ±19%) and 10% (p=0.655, acceptability at 95%: +11%/-9%), respectively (Figure 1).

TABLE 3. Linear mathematical models of adjustment for the measurement of the spirometric parameters FVC, FEV1, and FEV1/FVC from the power determinations of the frequency segments.

Impedance Modulus Equations $y = Ax + B$					Impedance Phase Equations $y = Ax + B$				
Dep.V (y)[1]	*Indep.V* (x)[2]	Coefficients A	Coefficients B	R^2	Dep.V (y)[1]	*Indep.V* (x)[2]	Coefficients A	Coefficients B	R^2
FVC	S7_25%[3]	-173	115	0.5	FVC	PhS4_25%[7]	-80	92	0.1
	S7_50%[4]	-329	175	0.7		PhS4_75%[8]	100	29	0.3
	S7_75%[5]	148	9	0.6		PhS7_25%[9]	-155	109	0.5
FEV1	S7_50%[4]	-233	120	0.4		PhS7_75%[10]	111	23	0.5
FEV1/FVC	S2_75%[6]	-33	65	0.5	FEV1	PhS4_25%[7]	-90	70	0.2
						PhS4_75%[8]	88	11	0.4

[1] Dep.V: Dependent variable of the linear equation.
[2] *Indep.V*: Independent variable of linear equation.
[3] Quartile at 25% of impedance module power determinations from Segment 7 (939.95 mHz – 1.06 Hz)
[4] Quartile at 50% of impedance module power determinations from Segment 7 (939.95 mHz – 1.06 Hz).
[5] Quartile at 75% of impedance module power determinations from Segment 7 (939.95 mHz – 1.06 Hz).
[6] Quartile at 75% of impedance module power determinations from Segment 2 (156.66 – 274.15 mHz).
[7] Quartile at 25% of impedance phase power determinations from Segment 4 (469.98 – 587.47 mHz).
[8] Quartile at 75% of impedance phase power determinations from Segment 4 (469.98 – 587.47 mHz).
[9] Quartile at 25% of impedance phase power determinations from Segment 7 (939.95 mHz – 1.06 Hz)
[10] Quartile at 75% of impedance phase power determinations from Segment 7 (939.95 mHz – 1.06 Hz).

TABLE 4. Evaluation of the mathematical linear fit models (y = Ax + B) for the estimation of the spirometric parameters FVC, FEV1, and FEV1/FVC.

Evaluation of the calibration equations of the impedance module					
Parameter	***Indep.V (x)*[1]**	**Estimation[2]**	**Correlation[3]**	**Error (%)[4]**	**P-value (T-Student)[5]**
FVC	S7_25%[6]	70 ± 10	0.72 (p = 0.002)	12 ± 7	0.937
	S7_50%[7]	70 ± 11	0.81 (p < 0.001)	10 ± 6	0.926
	S7_75%[8]	71 ± 11	0.76 (p = 0.001)	12 ± 6	0.847
FEV1	S7_50%[7]	46 ± 8	0.65 (p = 0.009)	19 ± 14	0.957
FEV1/FVC	S2_75%[9]	45 ± 5	0.69 (p = 0.005)	10 ± 5	0.655
Evaluation of impedance phase calibration equations					
Parameter	***Indep.V (x)*[1]**	**Estimation[2]**	**Correlation[3]**	**Error (%)[4]**	**P-value (T-Student)[5]**
FVC	PhS4_25%[10]	70 ± 5	0.33 (NS)	15 ± 9	1.000
	PhS4_75%[11]	70 ± 8	0.55 (p = 0.032)	13 ± 7	0.983
	PhS7_25%[12]	70 ± 9	0.68 (p = 0.005)	12 ± 9	0.902
	PhS7_75%[13]	71 ± 10	0.68 (p = 0.005)	12 ± 9	0.824
FEV1	PhS4_25%[10]	45 ± 5	0.42 (NS)	21 ± 16	0.928
	PhS4_75%[11]	47 ± 7	0.65 (p = 0.009)	19 ± 17	0.542

[1] Independent *Variable (x)* of the adjustment equation. See Table 3.
[2] Estimation of the spirometric parameters from the adjustment equations, see Table 3.
[3] Pearson's correlation between the theoretical spirometric parameters and those estimated with the adjustment equations, see Table 3.
[4] Error percentages of the values estimated with the calibration models of Table 3.
[5] Student's t test statistical p-value.
[6] Quartile at 25% of impedance module power determinations from Segment 7 (939.95 mHz – 1.06 Hz).
[7] Quartile at 50% of impedance module power determinations from Segment 7 (939.95 mHz – 1.06 Hz).
[8] Quartile at 75% of impedance module power determinations from Segment 7 (939.95 mHz – 1.06 Hz).
[9] Quartile at 75% of impedance module power determinations from Segment 2 (156.66 – 274.15 mHz).
[10] Quartile at 25% of impedance phase power determinations from Segment 4 (469.98 – 587.47 mHz).
[11] Quartile at 75% of impedance phase power determinations from Segment 4 (469.98 – 587.47 mHz).
[12] Quartile at 25% of impedance phase power determinations from Segment 7 (939.95 mHz – 1.06 Hz).
[13] Quartile at 75% of impedance phase power determinations from Segment 7 (939.95 mHz – 1.06 Hz).

The correlation between baseline and estimated measurements for FVC and FEV1 was approximately 64% ($p < 0.05$) and 65% ($p < 0.01$), respectively (Table 4). The mean value of the dispersion of the FVC and FEV1 measurements obtained with a spirometer and those estimated using the impedance phase adjustment equations (Table 3) were approximately 13% (mean value of p, 0.927, acceptability at 95%: ±23%) and 20% (mean p-value, 0.735, acceptability at 95%: 20%/-21%) (Figure 2).

The objective of this study was to obtain a set of mathematical calibration models that would allow adjusting the frequency powers of the module and the phase of the impedance changes obtained by EIT to estimate the FVC, FEV1, and FEV1/FVC parameters.

The technique implemented to process the changes in impedance was the analysis of the implicit frequency components of the same ventilatory impedance signal. Unlike a pneumotachometer that only records airflow variations, the EIT can detect small variations that originate in the lung parenchyma due to air circulation. These are detected by the penetration of the electrical injection current through the thoracic tissue [18] and are evidenced as a carrier or parasitic signals with different amplitudes and frequencies implicit in the signal.

From the analysis of the impedance module and the three spirometry parameters, correlations of approximately 70% were evidenced. The FVC correlated with the three quartiles of segment 7 and 3 adjustment equations were obtained with a mean value of R^2 of 60% and with a mean correlation between determinations (measured and estimated) of 76% (error: 11%, p: NS). FEV1 correlated with the quartile at 50% of segment 7, an equation was obtained with an R^2 of 40% with a correlation between measurements of 65% (error: 20%, p: NS). And the FEV1/FVC ratio with the quartile at 75% of segment 2, an equation with an R^2 of 50% and a correlation of 60% was obtained (error: 10%, p: NS).

Bland and Altman plots to estimate FVC from the modulus powers of the impedance signal

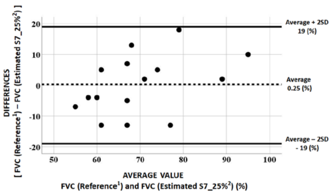

Fig. 1.1 Estimated FVC S7_25%

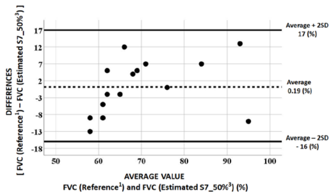

Fig. 1.2 Estimated FVC S7_50%

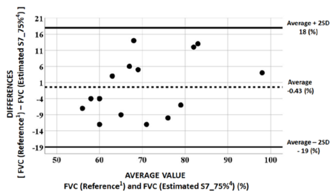

Fig. 1.3 Estimated FVC S7_75%

Bland and Altman plots to estimate FEV1 from the modulus powers of the impedance signal

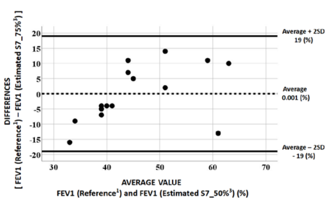

Fig. 1.4 Estimated FEV1 S7_50%

Bland and Altman plots to estimate FEV1/FVC from the modulus powers of the impedance signal

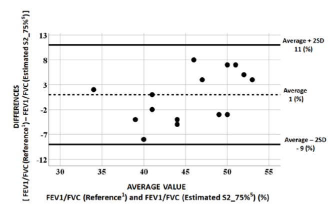

Fig. 1.5 Estimated FEV1/FVC S2_75%

[1]FVC, FEV1, and FEV1/FVC parameters measured with a spirometer.
[2]Adjustment equation to estimate FVC determined by the quartile at 25% of the data corresponding to segment 7 (Table 3).
[3]Adjustment equation to estimate FVC determined by the quartile at 50% of the data corresponding to segment 7 (Table 3).
[4]Adjustment equation to estimate FVC determined by the quartile at 75% of the data corresponding to segment 7 (Table 3).
[5]Adjustment equation to estimate FEV1/FVC determined by the quartile at 75% of the data corresponding to segment 2 (Table 3).

FIGURE 1. Analysis of differences in spirometric parameters (FVC, FEV1, and FEV1/FVC) obtained using spirometry equipment and those obtained based on the powers of the impedance change module obtained using an electrical impedance tomography system.

From the analysis of the frequency spectrum of the phase and the spirometry parameters, the FVC and FEV1 showed significant correlations of approximately 60%. The FVC with the Q25% and Q75% quartile of segments 4 and 7, respectively. Four equations were obtained with a mean R2 of 35% and a correlation between determinations of 64% (error: 13%, p: NS). Finally, the FEV1 with the quartiles at 25% and 75% of segment 4, two mathematical models were obtained with a mean R2 of 30%, and a correlation between determinations of 54% (error: 20%, p: NS).

Other research groups have proposed various techniques to process EIT changes. The parameters derived from the processing have been correlated with the spirometry parameters. Milne *et al.* [19] propose to characterize ventilatory heterogeneity (HV) from a series of estimated parameters of the changes in circulating volume obtained by means of EIT. Five determinations were obtained from each element of the EIT images: 1) half-expiratory time (tE), 2) the average difference between the temporal impedance changes of each pixel and the impedance variations corresponding to the entire image (Phase), 3) the mean amplitude of the impedance changes (ΔZ), 4) the coefficient of variation (CV) and 5) the index of heterogeneity (IH). The CV was defined as the ratio of the standard deviation and the average of the impedance changes obtained in the entire EIT image.

The IH was estimated in a region of interest (ROI) of 25 pixels where the pixel of interest was located in the center of the ROI. The regional CV value is assigned to the pixel of interest. This value was defined as the

Bland and Altman plots to estimate FVC from impedance signal phase powers

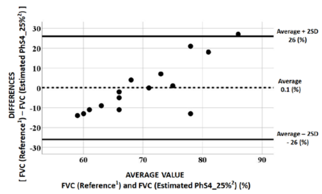

Fig. 2.1 FVC estimated PhS4_25%

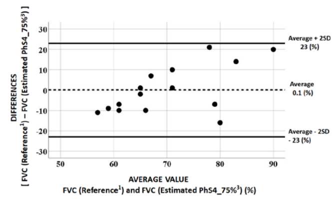

Fig. 2.2 FVC estimated PhS4_75%

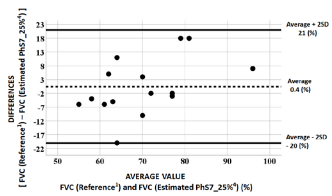

Fig. 2.3 FVC estimated PhS7_25%

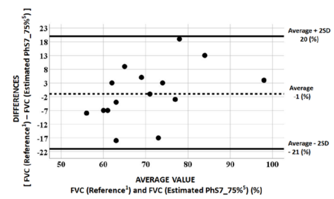

Fig. 2.4 FVC estimated PhS7_75%

Bland and Altman plots to estimate FEV1 from impedance signal phase powers

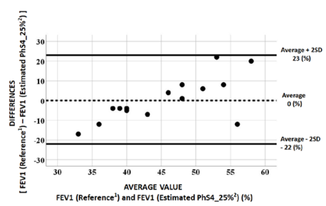

Fig. 2.5 FEV1 estimated PhS4_25%

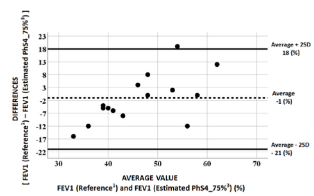

Fig. 2.6 FEV1 estimated PhS4_75%

[1] FVC, FEV1, and FEV1/FVC parameters measured by a spirometer.
[2] Adjustment equation to estimate FVC determined by the quartile at 25% of the phase powers of segment 4 (Table 3).
[3] Adjustment equation to estimate FVC determined by the quartile at 75% of the powers of the phase of segment 4 (Table 3).
[4] Adjustment equation to estimate FVC determined by the quartile at 25% of the powers of the phase of segment 7 (Table 3).
[5] Adjustment equation to estimate FVC determined by the quartile at 75% of the powers of the phase of segment 7 (Table 3).

FIGURE 2. Analysis of differences in spirometric parameters (FVC, FEV1, and FEV1/FVC) obtained using spirometry equipment and obtained based on the phase powers of impedance changes obtained using an electrical impedance tomography system.

Local Heterogeneity Score (LHS). The ROI then moves to its adjacent position and starts the regional CV estimation and LHS assignment again. The estimation cycle ends when the LHS is assigned to each pixel of the image. From the results obtained based on the Phase of the EIT impedance signal, a correlation between FEV1 and the CV and IH parameters of r = -0.59 (p = 0.01) and r = -0.53 (p = 0.02) was evidenced, respectively. And a correlation between FEV1/FVC and CV and IH parameters of r = -0.4 (p = 0.03) and r = -0.38 (p = 0.1), respectively [19]. Lasarow *et al.* [20] propose the use of EIT for monitoring forced pulmonary ventilation using regions of interest and for estimating the parameters used in [19], CV and IH. Correlations between FVC and CV and IH parameters of r = -0.1515 (p = 0.0903) and r = -1534 (p = 0.0864), respectively, were evidenced. From the analysis of FEV1 and the CV and IH parameters, a correlation of r = -0.2758 (p = 0.0018) and r = -0.2799 (p = 0.0015) was evidenced, respectively [20].

The comparison of the results obtained in [19], [20] and those obtained in this study are shown in Table 5.

TABLE 5. Comparison of results obtained between research groups.

	Milne *et al*. (2019) [19][1]		Lasarow *et al*. (2021) [20][2]		Present study	
Parameters	CV[3]	HI[4]	CV[3]	HI[4]	TRF-Module[5]	TRF-Phase[6]
FVC			-0.15 (p=0.0903)	-0.15 (p=0.0864)	0.76 ($p<0.05$)	0.64 ($p<0.05$)
FEV1	-0.59 (p=0.01)	-0.53 (p=0.02)	-0.28 (p=0.0018)	-0.28 (p=0.0015)	0.65 ($p<0.05$)	0.54 ($p<0.05$)
FEV1/FVC	-0.40 (p=0.03)	-0.38 (p=0.1)			0.60 ($p<0.05$)	

The results obtained in this study were significantly superior to those found by Milne *et al.* [19] by 6% and 34% for FEV1 and FEV1/FVC, respectively. And those found by Lasarow *et al.* [20] in 79% and 53% for the FVC and FEV1 parameters, respectively.

The next step of the investigation will be to find a relationship between the spirometry parameters and the impedance changes using an array of four electrodes. This study will demonstrate the feasibility of using simpler and less expensive impedance equipment to be used in the clinical field on an outpatient basis.

CONCLUSIONS

EIT impedance changes due to pulmonary ventilation are composed of signals of different amplitudes and frequencies that are the result not only of chest movements but also of the behavior of the lung parenchyma conditioned by the flow of circulating air. These frequencies correlate with the spirometry parameters FVC, FEV1, and FEV1/FVC. FVC and FEV1 show a statistically significant correlation in the frequency range between 939.95mHz and 1.06Hz and FEV1/FVC in the range between 156.66mHz - 274.15mHz. The calibration equations conditioned by each frequency component and intended for the estimation of the spirometry parameters showed a sufficient mathematical adjustment to obtain estimates comparable to those of the reference values. This monitoring technique could be used in patients to determine the degree of pulmonary obstruction/restriction non-invasively and only with monitoring of circulating volume.

AUTHOR CONTRIBUTIONS

F. M. V. L. conceptualized the project, curated data, developed the methodology, carried out formal analyses, performed bibliographical research and investigated in order to carry out the project, and participated in the writing of the original manuscript. S. K. conceptualized the project, curated data and validated, carried out formal analyses, developed the methodology, participated in the writing, reviewing and editing the manuscript. P. J. R. C. performed bibliographical research and investigation for the project and validated data, developed the methodology, performed bibliographical research and investigation, and participated in the writing, reviewing and editing the manuscript. P. C. C. performed bibliographical research and investigation for the project, developed the methodology, performed bibliographical research and investigation and validated data, participated in the writing, reviewing and editing the manuscript. J. M. B. O. conceptualized the project, curated data, developed the methodology, performed bibliographical research and investigation for the project, provided funding, oversaw the general progress of the project and provided resources, contributed to writing the draft and final version of the manuscript, reviewed and edited comments. All authors reviewed and approved the final version of the manuscript.

Ethical statement

This study was approved by the Ethical Committee of the University of Guanajuato with code CIBIUG-A56-2019.

REFERENCES

[1] Instituto Nacional de Estadística, Geografía e Informática (INEGI). Mortality dataset, distributed by INEGI. [Internet]. 2022. Available from: *https://www.inegi.org.mx/programas/mortalidad/#Tabulados*

[2] Global Initiative for Chronic Obstructive Lung Disease. 2022 Gold Reports [Internet]. 2022. Available from: *https://goldcopd.org/wp-content/uploads/2021/12/GOLD-REPORT-2022-v1.1-22Nov2021_WMV.pdf*

[3] Halpin DMG, Criner GJ, Papi A, Singh D, et al. Global Initiative for the Diagnosis, Management, and Prevention of Chronic Obstructive Lung Disease. The 2020 GOLD Science Committee Report on COVID-19 and Chronic Obstructive Pulmonary Disease. Am J Respir Crit Care Med [Internet]. 2021;203(1):24-36. Available from: **https://doi.org/10.1164/rccm.202009-3533SO**

[4] Virani A, Baltaji S, Young M, Dumont T, et al. Chronic Obstructive Pulmonary Disease: Diagnosis and GOLD Classification. Crit Care Nurs Q [Internet]. 2021;44(1):9-18. Available from: **https://doi.org/10.1097/CNQ.0000000000000335**

[5] Hernández-Ruiz A, Ortega HJ, Aguirre-Acevedo DC. Utilidad de la espirometría en los pacientes hospitalizados por la enfermedad pulmonar obstructiva crónica (EPOC) exacerbada. Iatreia [Internet]. 2020;33(4):341-347. Available from: *https://revistas.udea.edu.co/index.php/iatreia/article/view/339541*

[6] Zhao Z, Fu F, Frerichs I. Thoracic electrical impedance tomography in Chinese hospitals: a review of clinical research and daily applications. Physiol Meas [Internet]. 2020;41(4):04TR01. Available from: **https://doi.org/10.1088/1361-6579/ab81df**

[7] Karagiannidis C, Waldmann AD, Róka PL, Schreiber T, et al. Regional expiratory time constants in severe respiratory failure estimated by electrical impedance tomography: a feasibility study. Crit Care [Internet]. 2018;22(1):221. Available from: **https://doi.org/10.1186/s13054-018-2137-3**

[8] Vogt B, Zhao Z, Zabel P, Weiler N, et al. Regional lung response to bronchodilator reversibility testing determined by electrical impedance tomography in chronic obstructive pulmonary disease. Am J Physiol Lung Cell Mol Physiol [Internet]. 2016;311(1):L8-L19. Available from: **https://doi.org/10.1152/ajplung.00463.2015**

[9] Tang Y, Turner MJ, Yem JS, Baker AB. Calibration of pneumotachographs using a calibrated syringe. J Appl Physiol [Internet]. 2003;95(2):571-576. Available from: **https://doi.org/10.1152/japplphysiol.00196.2003**

[10] de Lema B, Casan P, Riu PJ. Electrical Impedance Tomography: Standardizing the Procedure in Pneumology. Arch Bronconeumol [Internet]. 2006;42(6):299-301. Available from: **https://doi.org/10.1016/s1579-2129(06)60146-8**

[11] Balleza Ordaz JM. Monitorización del patrón ventilatorio (PV) mediante tomografía por impedancia eléctrica (TIE) en paciente con enfermedad pulmonar obstructiva crónica (EPOC) [Ph.D.'s thesis]. [Cataluña]: Universitat Politèctica de Catalunya, 2012. 261p. Spanish. Available from: *https://upcommons.upc.edu/bitstream/handle/2117/94737/TJBO1de1.pdf;jsessionid=A8A27A61BBD1417D29C2D0179ED3DAAC?sequence=1*

[12] Serrano RE, de Lema B, Casas O, Feixas T, et al. Use of electrical impedance tomography (TIE) for the assessment of unilateral pulmonary function. Physiol Meas [Internet]. 2002;23(1):211. Available from: **https://doi.org/10.1088/0967-3334/23/1/322**

[13] Casas O, Rosell J, Bragós R, Lozano A, et al. A parallel broadband real-time system for electrical impedance tomography. Physiol Meas [Internet]. 1996;17(4A):A1. Available from: **https://doi.org/10.1088/0967-3334/17/4A/002**

[14] Phyton, version 3.10 [Internet]. Python Software Foundation; 2022. Available from: *https://www.python.org/downloads/release/python-3104/*

[15] Smith SW. The Scientist and Engineer's Guide to Digital Signal Processing [Internet]. San Diego: California Technical Publishing; 1999. Available from: *https://www.dspguide.com/*

[16] Weeks M. Digital Signal Processing: using MATLAB and wavelets. Massachusetts: Jones & Bartlett Learning; 2007. 492p.

[17] Braždžionytė J, Macas A. Bland-Altman analysis as an alternative approach for statistical evaluation of agreement between two methods for measuring hemodynamics during acute myocardial infarction. Medicina [Internet]. 2007;43(3):208. Available from: **https://doi.org/10.3390/medicina43030025**

[18] Grimnes S, Martinsen OG. Bioimpedance and bioelectricity basics [Internet]. Oxford: Academic Press; 2008. 488p. Available from: *https://www.sciencedirect.com/book/9780123740045/bioimpedance-and-bioelectricity-basics*

[19] Milne S, Huvanandana J, Nguyen C, Duncan JM, et al. Time-based pulmonary features from electrical impedance tomography demonstrate ventilation heterogeneity in chronic obstructive pulmonary disease. J Appl Physiol [Internet]. 2019;127(5):1441-1452. Available from: **https://doi.org/10.1152/japplphysiol.00304.2019**

[20] Lasarow L, Vogt B, Zhao Z, Balke L, et al. Regional lung function measures determined by electrical impedance tomography during repetitive ventilation maneuvers in patients with COPD. Physiol Meas [Internet]. 2021;42:015008. Available from: **https://iopscience.iop.org/article/10.1088/1361-6579/abdad6**